

Degradation Assessment of LDPE Multilayer Films Used as a Greenhouse Cover: Natural and Artificial Aging Impacts

Abdelkader Dehbi,¹ Abdel-Hamid I. Mourad,² Amar Bouaza¹

¹Engineering Physics Laboratory, University Ibn Khaldoun, Bp 78 Zaaroura, 14000 Tiaret, Algeria

²Faculty of Engineering, Mechanical Engineering Department, United Arab Emirates University, Al-Ain, United Arab Emirates

Received 26 January 2011; accepted 16 May 2011

DOI 10.1002/app.34928

Published online 3 November 2011 in Wiley Online Library (wileyonlinelibrary.com).

ABSTRACT: This article focuses on the assessment and understanding of the mechanism of natural and artificial aging processes of a triple-layer film made of low-density polyethylene (LDPE) used as greenhouse cover. The film material contains color dye and ultraviolet-A (UV-A) and infrared (IR) stabilizers and antioxidant. The combined effect of temperature variations and UV-A radiations, of the natural and artificial aging, on the physical properties (free surface energy and yellow color measurements), mechanical behavior (tensile tests), thermal stability (TGA and DSC analysis), and structural stability (FTIR analysis) was investigated. The natural aging was conducted on a greenhouse, located in northern Algeria, over a period of 7 months. However, the artificial aging was performed at four different agricultural greenhouse simulating conditions of temperature and UV-A radiation (namely, at 40°C, 40°C with UV-A, 50°C, and 50°C with UV-A) for periods of aging up to 5486 h (7.6 months). The results revealed that, the maximum loss of the yellow color addi-

tives occurs at 2981 h under the natural aging process and at 2440, 1096, 1340, and 121 h under the four artificial aging conditions, respectively. There was an observed increase in the films free surface energy and a significant degradation in the mechanical properties with aging time. This can be correlated with the film material structural changes. The natural aging of the film in North Africa is almost equivalent to artificial aging at 40°C. The concurrent effect of temperature and UV-A radiations induced polymer chains scission leading to faster degradation in the film material and consequently a reduction in its durability and service lifetime. The results show also that the measured parameters are directly related to the limit of use criterion for evaluating the lifespan of agricultural greenhouse LDPE covers. © 2011 Wiley Periodicals, Inc. *J Appl Polym Sci* 124: 2702–2716, 2012

Key words: tri-layer LDPE film; greenhouse; natural and artificial aging; degradation; lifetime; UV-A

INTRODUCTION

Nowadays, the use of three-layer co-extrusion technology achieves quality plastic films for greenhouse covers. Low-density polyethylene LDPE is one of the most used materials in plasticulture and its utilization as agricultural greenhouse covers is a common application. The main properties that have ensured its success are especially its lightness and transparency. However, despite its good chemical inertness, like polyethylene all organic substances degrades slowly under the combined influence of heat, solar ultraviolet UV radiation, mechanical stress, and chemical agents.^{1–6} Sunlight is the primary detrimental factor in the aging of greenhouse. The antioxidants protect the film from the harmful effect of UV radiation and heat for long periods. A large number of additives are currently available and when added in low concentration to polymers make them more

stable under exposition to heat and UV radiations. This enabled a considerable number of possible formulations of polyethylene films to be synthesized with adapted properties to be more suitable for their applications. Nevertheless, the degradation mechanism of PE is yet not well understood.⁷ Polyethylene (PE) environmental degradation is a complex process, as many degradation mechanisms act together toward the total destruction of the material.

Sigbritt et al.⁸ have investigated the degradation products formed during photo-oxidation and low-temperature thermo-oxidation in a 30 μm thick polyethylene film (LDPE). The films were photo-oxidized with UV lamps. Samples were irradiated for different amounts of time up to 300 h. Similar materials were also subjected to thermal aging at 80°C. The degradation rate and molecular weight changes were compared and correlated with the identified degradation products. They have observed that the number-average molecular weight (M_n) and weight average molecular weights (M_w) of LDPE decreased during the UV radiation. They have discussed such degradation in the M_n and M_w in terms of different photo-oxidation times. Table I gives the molecular

Correspondence to: A.-H. I. Mourad (ahmourad@uaeu.ac.ae).

TABLE I
The Molecular Weight (Average Number M_n and Average Weight M_w) of Unaged and Aged LDPE⁸

Degradation procedure	M_n	M_w
Unaged	34,700	189,000
After 5 weeks at 80°C	35,900	188,000
After 100 h of UV	18,700	149,000
After 100 h of UV+ 5 week at 80°C	12,700	62,400

weights after thermal and UV-initiated thermal aging at 80°C. It decreased slowly during 5 weeks at 80°C. While it decreased rapidly during 100 h of irradiation. When 100 h of photo-oxidation was followed by 5 weeks at 80°C, the material experienced further degradation. The reflection FTIR was used by Sigbritt et al.⁸ to examine the surfaces of degraded polymers and in particular the initial product formation. The variation of the carbonyl absorbance measured at 1718 cm^{-1} as a function of irradiation time for the different was obtained. The results showed that the concentration of carbonyl groups at the surface increases at prolonged irradiation times. They have observed a good correlation between the molecular weights and carbonyl index. The samples that showed the largest decrease in molecular weight had the highest carbonyl index. The amount of products formed agreed well with changes in the molecular weight and carbonyl index. As the photo-oxidation time increased, larger amounts of low molecular weight products were produced.

Briassoulis and Waaijbergen⁹ have attempted to collect and compare the standards of plastic films for use as greenhouse cover. They have noted about the disparity of the results and the lack of coordination in the field of greenhouse covering.^{10–12} The Existing standards are not generalized and unified. In fact, they are adapted to serve for the local conditions in the developing countries and therefore, inappropriate for application or use in particular conditions.

The duration of use of plastic materials is relatively short compared to their life time. It ranges from several months to few years, depending on the conditions of use and environment. The degradation of polymers in outdoor use is mainly due to UV radiations of the solar spectrum.^{13–15} Mourad et al.^{3,4} reported about the severe effect of UV radiation and some of the environmental conditions on the thermo-mechanical properties of PE. Some researches have investigated the long-term behavior of polyethylene films. Hassini et al.¹⁶ have studied the effect of simulated sand wind during 4 h on a polyethylene film. They have showed that the sand wind creates, on the exposed surface of the film, a very thin layer encrusted with sand particles producing a phenomenon of impact. Dilara and Briassoulis¹⁷ showed that the durability of the film material depends on its abil-

ity to resist erosion. The effect of some aging parameters (e.g., heat, UV radiation) on the mechanical, thermal, and structural stability and degradation behavior of different grades of PE was investigated by Mourad et al.^{1–6}

The degradation behavior of mono-layer LDPE films used as greenhouse covers was studied by many authors. However, the degradation behavior of multi-layer films is very lacking. Few studies^{18,19} have considered the effect of aging in the North-Africa climatic conditions. Adam et al.¹³ have studied the behavior of polymeric greenhouse covers made of a sandwich structure of three layers, one EVA19 layer inserted between two low-density polyethylene layers. Optical, thermal, surface analysis and mechanical properties were analyzed on samples having undergone different thermal treatments associated with sand and wind simulation.

In the light of the above the effect of aging conditions on the behavior of multi-layered LDPE films needs more attention. In the current work the degradation behavior of tri-co-extruded layers LDPE film used as agricultural greenhouse cover was investigated under both natural and artificial aging. In the natural aging, there are many weathering or climatic conditions behind the deterioration of the properties of greenhouse cover. Among these, climatic parameters are solar irradiation, temperature, humidity and rainfall, snowfall, hail, and wind. In the artificial aging, the film was exposed to the most deteriorative parameters, that is, temperature and UV-A radiation. These aging climatic parameters are considered the most responsible parameter for aging of agricultural greenhouse covers in the regions of North Africa and the Sahara.

The main aim of this work is to contribute to broad the pool of the available data and information for the adaptation of plastic films used as greenhouse cover in the regions of North-Africa and the Sahara. To accomplish this study, the LDPE film has undergone natural and artificial aging processes. In the natural aging the film was exposed to the climate of northern Algeria. In the artificial aging the film was exposed to four different combined and simultaneous conditions of temperatures and UV-A radiations. These are 40°C, 40°C with AV-A radiation, 50°C and 50°C with UV-A radiations. The exposure was performed over a time period ranging from 0.0 to 5486 h (7.6 months). This study could be extended to cover more areas with different environmental conditions to establish a generalized standard

EXPERIMENTATIONS

Materials

The employed LDPE film was manufactured by Agrofilm SA (Setif-Algeria) using the three-layer co-

TABLE II
Different Aging Periods

Time (h)	10	100	500	750	1000	2000	2480	3000	5250	5486
Time (Month)	0.014	0.14	0.67	1.04	1.39	2.78	3.44	4.17	7.29	7.62

extrusion technology. The total thickness of the three co-extruded layers film is 180 μm with the proportions of $1/4$, $1/2$, and $1/4$ in the layers. The raw LDPE (before extrusion) has density of 0.923 g/cm^3 and the weight average molecular weight is in the range of 90,000–120,000. The melt flow index MFI of the raw LDPE and stabilizer are 0.33 g/10 min and 10 g/10 min, respectively. The initial color of the film is milky yellow. The real composition of the film is not known (kept confidential by the supplier). The usually used greenhouse cover is made from a mono-layer film with 180 μm , same as the overall thickness of the tri-layers film LDPE film. Self adhesion between the three co-extruded layers occurs under an extrusion temperature of 70°C .

Methodology

The study was conducted over a period of time ranging from 0.0 to 5486 h (7.6 months) under natural and artificial aging. Approximately 6% of the total solar radiation falling on the earth is ultraviolet. The UV is normally sub-divided into UV-A, UV-B, and UV-C radiation with wavelength ranges of 315–380 nm, 280–315 nm, and 100–280 nm, respectively. The artificial aging was conducted at four different conditions (40°C , 40°C with UV-A radiations, 50°C and 50°C with UV-A radiations). These are the most simulating climatic parameters for the agricultural greenhouse climatic conditions in North Africa. Table II presents the different periods of aging in months, days, and hours. The natural aging was conducted over a time period starting from March up to September with the climatic conditions shown in Table III.

The process of artificial aging was conducted in especially design and constructed weathering chamber. The chamber is equipped with UV-A lamp and fully controlled heating system. It is sealed and isolated properly to ensure proper degradation procedures. The relative humidity was maintained at 70%, which is equivalent to the average of the natural humidity over the total natural aging period (see Table

III). The LDPE films were photo-oxidized with UV-A lamp of 40 W power (Philips: TL-K 40W UV-A). This lamp gives radiation with wavelengths range of 315–380 nm (equivalent to that of the UV-A of the solar radiation). The distance between the lamp and the sample is 40 cm. samples were irradiated for the different amounts of time. Similar materials were also subjected to thermal aging at the different temperatures and times.

A greenhouse of 32 m length, 8 m width, and 3.50 m height was specially design, built, and equipped with a tri-layer LDPE film of 180 μm total thickness. The greenhouse was located in the neighborhood of Oran region of Algeria at $31^\circ 40' \text{ N}$ latitude, $00^\circ 36' \text{ longitude}$ and 120 m altitude with an east/west orientation. The samples were taken from each side of the greenhouse roof to represent the north side film and south side film. The samples were taken every month over the total aging period.

To ensure the consistency in the results after time of testing, one large sample (30 mm \times 30 mm) was initially cut and then all required specimens for different experiments were then cut from it. To ensure the consistency in the results, a relatively large sample (30 mm \times 30 mm) was initially taken from the roof, after aging period, from which the required tests specimens were then cut.

The tensile tests were performed (according to ISO 527-3 standard) using a universal testing machine (Instron model 4301) with a load cell of 5 kN. All tests were performed at room temperature with a cross head speed of 50 mm/min and displacement controlled condition. The specimens used have the following dimensions: initial overall length = 180 mm, initial length between the jaws = 80 mm, width = 6.5 mm, and thickness = 180 μm . Figure 1 shows a photo of a typical tensile test prepared according to ISO 527-3.

When the tensile curves exhibit an initial linear relationship, the modulus of elasticity E is determined as the slope of the first portion of the tensile curve. This method was used in the present work. Sometimes the secant modulus method is usually

TABLE III
The Average Temperature T and Relative Humidity H During Natural Aging

Month	March	April	May	June	July	August	September
T_{aver} ($^\circ\text{C}$)	32.8	33.6	37.6	41.6	44.2	43.6	41.1
H_{aver} (%)	76.2	69.3	62.5	60.0	58.7	59.0	63.7

aver, average.

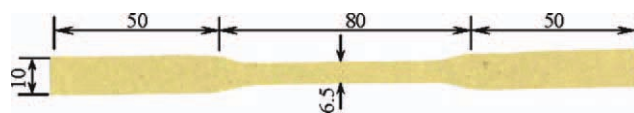


Figure 1 Photo of a typical tensile specimen (all dimensions in mm). [Color figure can be viewed in the online issue, which is available at wileyonlinelibrary.com]

employed when the stress–strain curve for a material does not exhibit linearity of stress to strain. In the absence of a distinct yield point, the yield strength can be determined by different techniques. Three different techniques were used here to determine the yield strength. In the first technique, it is determined as the point of the initial departure from linearity of the stress–strain curve, this is called the proportional limit. In the second technique, the yield strength is determined using 0.002 (or 0.2%) strain offset ($\sigma_{0.2}$). In this method, a straight line is constructed parallel to the elastic portion of the stress–strain curve at some specific strain offset of 0.002. The stress corresponding to the intersection of this line and the stress–strain curve as it bends over in the non linear region is defined as the yield strength at a strain offset of 0.002. In the third technique, the yield strength is determined as the stress at the point at which the curves becomes with zero gradient (at the first peak on the curve).

The study of surface tension is a significant element to determine the physicochemical interactions at the interface film/substrate. The presence of any chemical modifications in the film surface due to the effects of temperature and UV–A radiations were studied through the measurements of the free surface energy (surface polarization energy plus the triple-layer dispersion energy). The method is based on the measurement of the contact angle of different liquids (water and iodomethane). This is to evaluate the free dispersive interaction/component and non-dispersive or polar components of the free surface energy. Then the total free surface energy was obtained from the summation of the two components.

The contact angle θ is the angle between the outline tangent of a drop deposited on a planar solid and its surface.²⁰ Its value is a measure of the ability of a liquid to spread on a surface. The contact angle is linked to the surface energy and so one can calculate the surface energy and differentiate between polar and a polar interactions. Therefore, if several reference liquids are used, the surface energy of the solid can be calculated, discriminating between polar and dispersive components. The most common models are Good Van Oss model²¹ or Owens and Wendt model.²²

Three parameters influence the shape of a drop at solid surface. These are solid–liquid interfacial ten-

sion γ_{SL} , solid–vapor interfacial tension γ_{SV} (γ_S) and liquid–vapor interfacial tension γ_{LV} (γ_L). These three parameters are linked with the contact angle θ by the Young's equation:

$$-\gamma_{SV} + \gamma_{SL} + \gamma_{LV} \cdot \cos(\theta) = 0 \quad (1)$$

Solely, γ_{LV} and θ are measurable, so additional equations are necessary to determine γ_{SL} and γ_{SV} . Several models were developed to calculate these parameters (Owens and Wendt model). The OW model considers that the surface energy can be expressed as follows:

$$\gamma_S = \gamma_S^d + \gamma_S^p \quad (2)$$

where γ_S^d is the dispersive component (Lifshitz-Van der Waals interactions) and γ_S^p is non-dispersive component (polar interactions, Lewis acid-base).

The equation between tension components and contact angle is then:

$$\gamma_L(1 + \cos\theta) = 2\sqrt{\gamma_S^d \gamma_L^d} + 2\sqrt{\gamma_S^p \gamma_L^p} \quad (3)$$

where γ_L is the free surface energy, θ is the contact angle, indexes S and L stand for the solid and liquid phases, respectively, and the exponents d and p refer to disperse and polar components of the free surface energy. In this model the measure of contact angle of two different liquids with known dispersive and polar components are necessary to calculate the solid surface energy.

Three reference liquids were employed in this study. That is, ultra pure water (milli-Q Water System, resistivity 18 Ω/cm), glycerol (density 1.26 g/cm^3 and viscosity at 20°C is 9.34 $\text{g}/\text{cm}/\text{s}$) and iodomethane (density 3.325 g/cm^3 and solubility in water is 14 g/L at 20°C). All measurements were conducted at room temperature (23°C). For each liquid deposited on the simple surface, an average of five measurements was recorded. A drop of 3 mL, deposited with a micro syringe, was photographed with a black and white CCD camera (500 \times 500). Contact angle θ was determined using a computerized contact angle meter (NFT Communications Company, Tours, France).

The contact angle that the three liquids make on the sample surface was initially measured. Then according to the relationship proposed by Young and Dupre²³ and Fowkes²⁴ and with the Qwen Wendt model of Eq. (3),²² the samples free surface energy was calculated. Similar procedures were followed by Adam et al.¹³ and Sanchis et al.²⁵

Thermal analyses of the samples were performed using differential scanning calorimetry (DSC 2920 TA Instruments). Samples of ≈ 10 mg, was put in an

aluminum pan (drilled to facilitate the exchange of air between inside and outside). The samples were heated from ambient temperature up to 180°C with a heating rate of 10°C/min under nitrogen environment.

The color variations or modifications were measured using a color Reader CR10 Konica Minolta which records the percentage of yellow, red and blue colors.

The IR spectra were obtained with a FTIR spectrometer (Avatar 360), using ATR (attenuated total reflection) with a Ge crystal, by collecting and averaging 32 scans, at a resolution of 4 cm⁻¹. IR spectra are presented in reflection.

RESULTS AND DISCUSSION

Film free surface energy and color

The measurements of external free energy were performed on different films aged naturally (under a climate conditions of North Africa) and artificially at 40°C and 50°C with and without UV-A radiations. The variations of the free surface energy with aging time are presented in Figure 2.

In the natural aging, the samples were taken from each side of the greenhouse roof to represent the north and south sides. The natural aging curve shown is for the north side sample. The measured free surface energy of the unaged LDPE film is 30 mJ/m². This value is the expected one for LDPE film and was reported in the literature by Hassini et al.^{16,26} It can be seen that the free surface energy increases passing through a maximum value of ≈38.5 mJ/m² after 5 months (3600 h). There is an increase of 27% with respect to the free surface energy of unaged film. Then the value decreases to 33 mJ/m² at the end of natural aging period (5000

h/7 months). The curve of the south side sample has similar trend of the north side sample with maximum value of ≈40 mJ/m². Attaining the maximum value indicates the maximum loss of the yellow color additive. The decrease in the value may be due to the temperature drop ($T = 41.1^{\circ}\text{C}$) during the month of September.¹⁸

In the artificial aging the surface energy is constantly increasing up to the end of artificial aging period (5486 h/7.6 Months). The increase is proportional to the temperature; the values for 50°C are higher than that for 40°C. On the other hand, the increase is more influenced when the film is subjected to the combined action of the temperature and the UV-A radiations. The surface energy increases with aging time to a maximum of 42.26 mJ/m², 45.33 mJ/m², 50.77 mJ/m², and 54.57 mJ/m² for 40°C, 40°C + UV-A, 50°C and Δ 50°C + UV-A, respectively, at the end of artificial aging period (5486 h).

The film surface undergoes such essential modifications as the time of exposure increases because the various additives added during the formulation (anti-UV, anti-O₂, plasticizer, and yellow color additives) are able to diffuse from the bulk to the surface. Then, as the anti-UV additives have practically disappeared, the UV radiation and the associated oxidization reaction take place and dominate the aging process at the surface.

The LDPE is known to be a non polar material. However, during aging the LDPE, becomes a polar material this is due to the failure of polymer chains as a result of weathering/aging. Therefore, an increase in the surface energy was observed due to the increase of the non-dispersive (polar) part. The polar part of the surface energy is connected with the kinetics of free radicals in the top layer of LDPE and with oxygen-containing groups appearing due to oxidation in air; that characterize the degradation of LDPE.²⁶ Therefore, the observed increase in the film total free surface energy with aging time is due to free radicals of oxygen-containing groups, which are a measure for more cuts/scission of polymer chains (CH₂—CH₂) and consequently for the level of degradation. Similar observations were also reported by Adam et al.¹³ for greenhouse covers made from a sandwich structure of three layers, one EVA19 layer inserted between two LDPE layers.

The different carbonyl groups formed during oxidation of the LDPE materials (e.g., carboxylic acids, aldehydes, esters, ketones, and lactones) are more concentrated at the surface layers, because more oxygen is available near the surface. Many researchers, e.g., Sigbritt et al.,⁸ reported about the reduction in the PE molecular weight by photo degradation and/or thermal degradation. As aging time increases polymer of lower molecular weight formed during

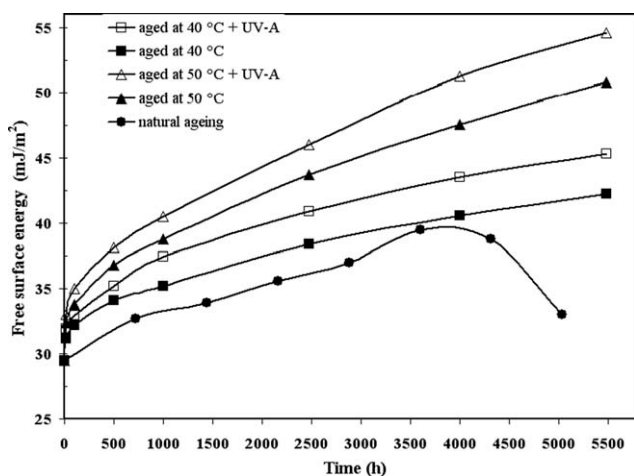


Figure 2 Variations of the free energy surface (mJ/m²) with the aging time (h) (● natural aging, ■ 40°C, □ 40°C + UV-A, ▲ 50°C, and △ 50°C + UV-A).

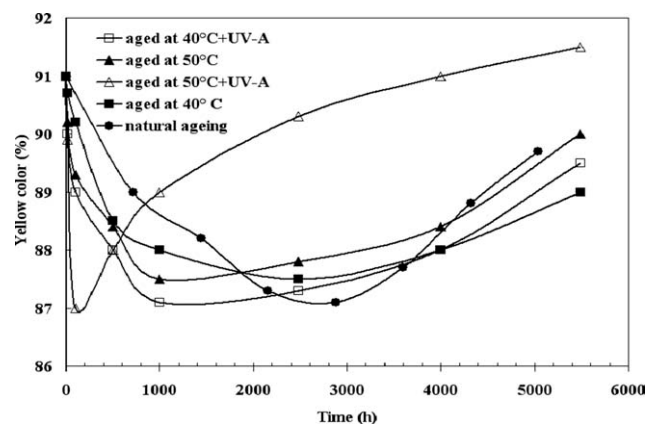


Figure 3 Evolution of the yellow color with the aging time (● natural, ■ 40°C, □ 40°C + UVA, ▲ 50°C, and △ 50°C + UVA).

photo-oxidation and or thermo-oxidation. Their results showed that, concentration of carbonyl groups at the surface increases at prolonged irradiation times and the increase in the photo-oxidation time produce larger amounts of low molecular weight products. A carboxyl radical at the end of the polyethylene chain formed either by decomposition of a secondary hydroperoxide followed by β -scission or by reaction of a primary alkyl radical at the chain end with oxygen can abstract a hydrogen intramolecularly from similar chain to form a carboxyl group and a secondary macroradical. The secondary alkyl radical can further react with oxygen to form a secondary hydroperoxide. As a result of the hydroperoxide decomposition, oxygen-containing groups are formed in the polyethylene chain. More details on the mechanism for the formation of degradation products are reported by Sigbritt et al.⁸ After the molecular weight of PE was reduced by photo degradation and/or thermal degradation, low molecular weight polymers are formed. This is a possible mechanism to explain the chain scission reaction and consequently the observed increase in the surface energy.

The percentage change in the yellow color of the LDPE film was measured as a function of time and presented in Figure 3. The percentage amount of the yellow color is 91% in the unaged film. At the beginning of aging there is usually a decrease in the value characterizing the yellow color with a passage through a minimum and then increases.

In the natural aging, the minimum value (86%) takes place at ~ 2981 h (4 months) then the curve increases without showing a plateau or steady state condition, even at the end of the 7 months of the natural aging. This indicates that the modifications in the color are continuing. The observed decrease is due to the disappearance of the yellow dye additives. The variation observed, during aging, in the

free surface energy can be correlated with the variation observed in the color (see Figs. 2 and 3). In fact, yellow color additives (which are mainly used to protect LDPE against irradiation) are not stabilized and migrate easily to the sample surface. This is the main change that occurs in the material during the first four or five months of aging. The minimum value means the maximum loss of the yellow color additives. The observed increase in the yellow color after 4 months was surprising and unexpected. It may be due to the decrease in the effect of sunlight. Scoptoni²⁷ showed that the UV light effects on a LDPE film (exposed under similar condition) are observable for an aging of 5 months. He explained that decreasing in the period is because of the washing mechanism of the roof surface due to rains. The increase in the intensity of the yellow color may be due to the degradation of the film.²⁷

Because of the artificial aging, the increase in the temperature (from 40 to 50°C) and exposure to UV-A radiations decrease the time of passage through the minimum. The results show that the maximum loss of the yellow color additive under the artificial aging at 40°C, 40°C + UV-A, 50°C, and 50°C + UV-A occurs at 2440, 1340, 1096, and 121 h, respectively. In sense the artificial aging reduces the time at which the additives maximum loss occurs by 18%, 55%, 63%, and 96% of that taken under the natural aging. The results of the change in the yellow color strengthen the results of the surface energy changes.

Mechanical behavior

The mechanical behavior of the unaged/virgin and naturally (up to a period of 5000 h/7 months) and artificially aged films (up to a period of 5486 h/7.6 month) was evaluated by conducting the tensile test. The load was applied on specimen in a direction parallel to the average molecular orientation obtained during the film processing. The engineering stress as a function of the engineering strain was recorded for each film. The tests were conducted to determine the tensile properties (modulus of elasticity E , yield strength σ_y , fracture stress σ_f , and elongation at break) of the material. A quantitative estimation of the effects of natural and artificial aging on the mechanical performances of the film is then done based on the knowledge of the measured properties.

Figures 4 and 5 show the stress-strain diagrams for naturally and artificially aged films, respectively. The curve for unaged film is also included in Figures 4 and 5 for the purpose of comparison. Four distinctive regions are observed in the tensile curves. The stress-strain diagrams for all samples increases almost linearly in the first (initial) region of the curve. The curve becomes nonlinear (in the second

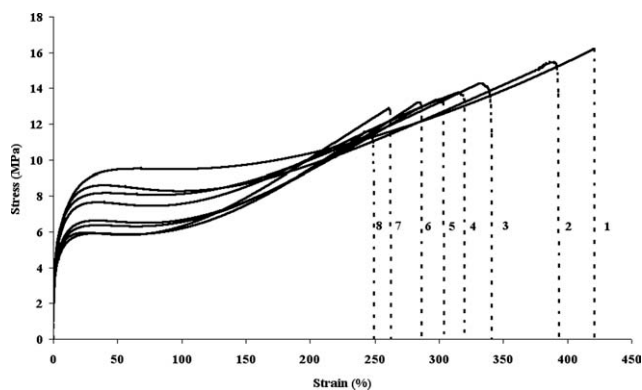


Figure 4 The stress–strain curve for unaged and naturally aged films: (1) unaged; (2) 1 month (720 h); (3) 2 months (1440 h); (4) 3 months (2160 h); (5) 4 months (2880 h); (6) 5 months (3600 h); (7) 6 months (4320 h); and (8) 7 months (5040 h).

region) with decreasing slope up to a point of zero gradient. Then the stress drops little to a constant drawing stress or becomes almost with zero gradient (in the third region) up to a certain engineering strain prior the work hardening starts and the stress increases again up to fracture (in the fourth region). All samples exhibit similar tensile behavior trend regardless the aging conditions.

As all tensile curves exhibit almost an initial linear relationship, the modulus of elasticity E is determined as the slope of the first portion of the tensile curve. The tensile behavior shows absence of a distinct yield point; therefore, the yield strength is determined by the three different techniques described in “Methodology.” Figures 4 and 5 show that, the unaged film has a higher level of stress than that of the aged films. Also, the achieved percent elongation for unaged film is higher than that of aged films and it reduces with aging time and exposure to UV radiation. Figure 6(a–c) present the

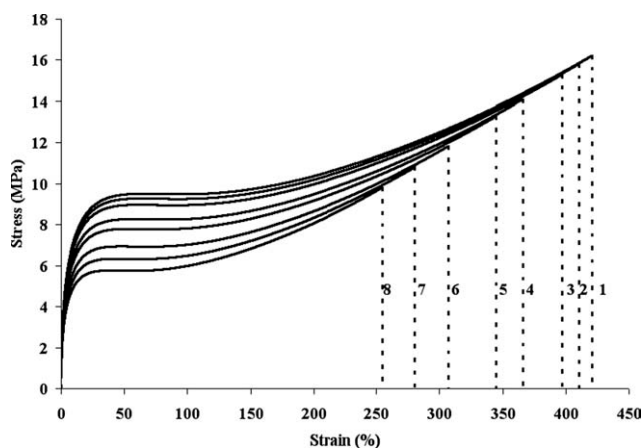


Figure 5 The stress–strain curve for unaged film and aged films at 40°C: (1) unaged film; (2) 20 h; (3) 100 h; (4) 500 h; (5) 1000 h; (6) 2480 h; (7) 4000 h; and (8) 5486 h.

variation of the tensile yield strength, measured based on the three mentioned methods, with aging time for different aging conditions. The tensile properties were initially measured for the tri-layers sheet made of virgin material. The measured yield strength (at the point of 0.0 gradient) is 9.6 MPa which equal to the value measured by Briassoulis et al.¹¹ for a monolayer LDPE sheet of 200 μm . A tensile fracture stress of 16 MPa was measured,

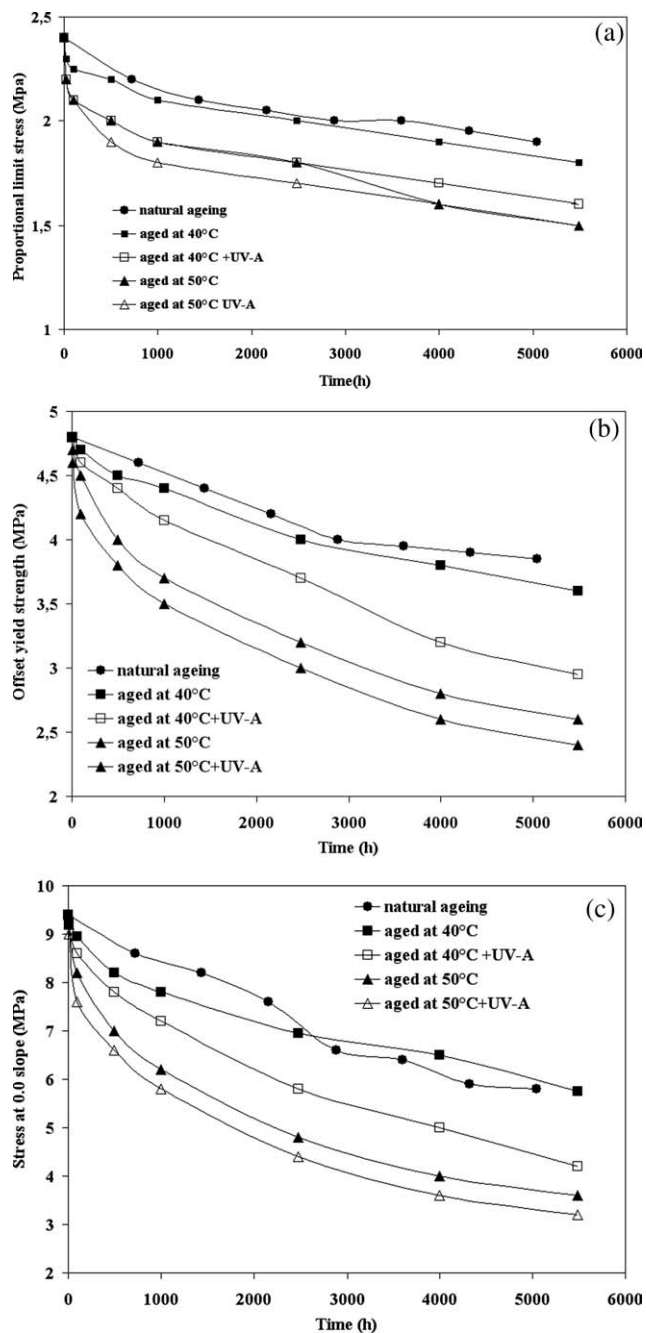


Figure 6 (a) Variation of yield strength (based on proportional limit method) with aging time. (b) Variation of yield strength (based on 0.2% offset strain) with aging time. (c) Variation of yield strength (at the point of zero gradient) with aging time.

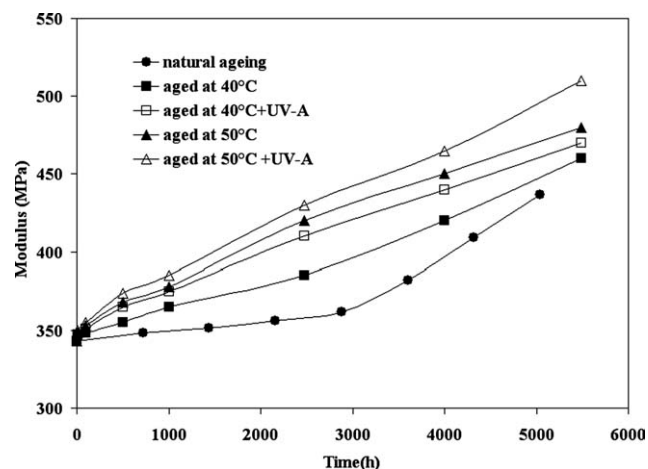


Figure 7 Evolution of the modulus of elasticity with the aging time (● natural, ■ 40°C, □ 40°C + UV-A, ▲ 50°C, and △ 50°C + UV-A).

which is of the order of what is expected for a monolayer of LDPE used in greenhouse technology. For instance Dilara et al.¹⁰ have measured values between 4.1 MPa and 15.6 MPa for a monolayer LDPE sheet of thickness between 50 μm and 200 μm . The yield strength (at the point of 0.0 gradient) after 5486 h of aging has values of 5.8 MPa, 5.75 MPa, 4.2 MPa, 3.6 MPa, and 3.2 MPa, under natural aging and artificial aging at 40°C, 40°C + UV-A, 50°C, and 50°C + UV-A, respectively. This shows that the yield strength of the unaged (9.6 MPa) material reduces by about 39.6%, 40.1%, 56.3%, 65.3%, and 66.7% under the five different aging conditions. The harshest effect is under the exposure to 50°C with UV-A radiation. This reflects the high rate of deterioration in the yield strength due to the investigated four aging conditions.

The yield strength of unaged film based on the proportional limit and 0.2% strain offset techniques are 2.4 MPa and 4.8 MPa, respectively. The values based on the proportional limit method at the end of the natural and the four artificial aging conditions are 1.9 MPa, 1.8 MPa, 1.6 MPa, 1.5 MPa, and 1.5 MPa, respectively. However, the values based on the 0.2% strain offset are 3.85 MPa, 3.6 MPa, 2.95 MPa, 2.6 MPa, and 2.4 MPa, respectively.

The yield strength measured by the three methods is essentially reduced with aging time. The highest degradation is for the aging under the exposure to the combined effect of 50°C with UV-A radiation. The yield stress values based on the 0.2% strain offset and on zero gradient point measurements techniques are almost double and triple the values based on the proportional limit technique, respectively. This means that the design based on the proportional limit yield strength is relatively conservative design.

The variation of the modulus of elasticity E with aging time is given in Figure 7. These values are calculated from the slope of the initial part of the curve. The value of the modulus of elasticity was found to be 340 MPa for unaged film. Dilara and Briassoulis¹⁰ have measured values between 96.5 and 262 MPa for LDPE sheets of thickness between 50 μm to 200 μm . Value between 100 MPa and 262 MPa were measured for monolayer LDPE film by several researchers.^{10–13,17,19,27,28} The values increase with aging time for the investigated five natural and artificial aging conditions. The trend of variation for natural and artificial aging at 40°C is similar. The variation is nearly bilinear and the rate of rise in the values is higher after ~ 3000 h of aging. The trend of variations for other three conditions is also bilinear, however, the rate of variation is little less after 500 h of aging. The modulus of elasticity after 5486 h of aging are 436 MPa, 460 MPa, 470 MPa, 480 MPa, and 510 MPa, under natural aging and artificial aging at 40°C, 40°C + UVA, 50°C, and 50°C + UV-A, respectively. The values have increased by about 27%, 34%, 37%, 40%, and 47% under the five different aging conditions if compared with the value of the unaged material. The highest increase was for the film exposed to UV-A radiation at 50°C condition.

Figure 8 shows the variation of the fracture stress with the aging time. The trend of variation resembles that for the yield strength. The fracture stress reduces with aging time and the harshest effect of aging was for exposure to UV-A radiation at 50°C. The maximum achieved fracture stress for unaged film is 16.2 MPa. Values of 12.2 MPa for natural aging and 9.82 MPa, 7.33 MPa, 6.11 MPa, and 5.59 MPa for artificial aging conditions at 40°C, 40°C + UV-A, 50°C, 50°C + UV-A, respectively, were achieved at the end of aging periods. In fact, the

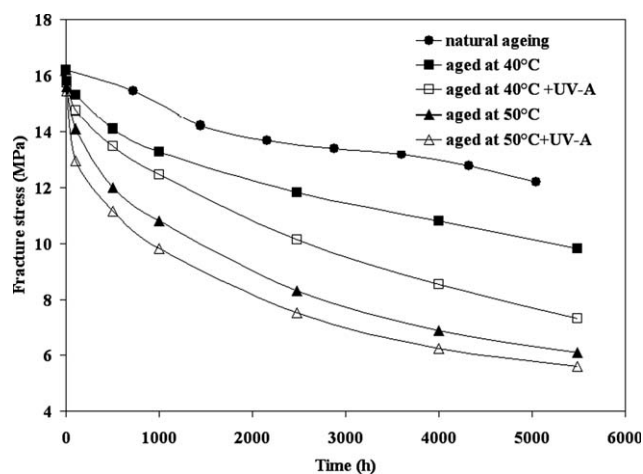


Figure 8 Variation of the fracture stress with aging time for different aging conditions.

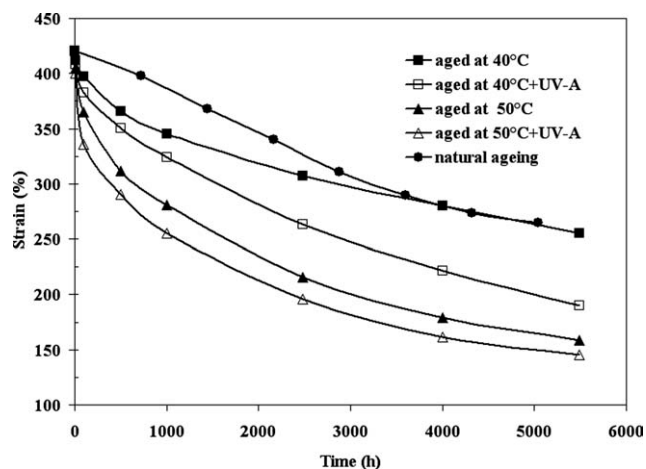


Figure 9 Evolution of the percent elongation with the aging time (● natural, ■ 40°C, □ 40°C + UV-A, ▲ 50°C, and △ 50°C + UV-A).

film material loses 25%, 40%, 55%, 62%, and 65%, respectively, of its initial fracture stress (in the unaged condition).

Figure 9 shows the variation of the elongation at break as a function of the aging time. The maximum achieved percent elongation of unaged material at break is 425% which reflects the ductile behavior of the virgin material. Briassoulis et al.¹² have reported a value of 550% for a monolayer of LDPE sheet of thickness 200 μm . The percent elongations after 5486 h of aging are 265%, 255%, 190%, 159%, and 145%, under natural aging and artificial aging at 40°C, 40°C + UVA, 50°C, and 50°C + UV-A conditions, respectively. This reveals that the material lost about 37%, 39%, 55%, 62%, and 65% of its initial percent elongation (in the unaged condition) under the five different aging conditions, respectively. Such reductions in the ductility reflect the deteriorative effect of the aging on the ductility of the material. The most deteriorative impact is for UV-A radiation at 50°C aging condition. It is also noted that the variation under the natural aging is very close to that of the artificial aging at 40°C.

Generally, the modulus of elasticity, percent elongation, yield strength, and fracture stress deteriorate with aging conditions and time. It is worth noting here that, the apparent rise in the modulus of elasticity with aging is considered a sort of degradation in the mechanical behavior not enhancement. As such rise is at the expense of ductility and the film becomes stiffer and with reduced flexibility. Such degradation in the mechanical behavior of the tri-layer film of LDPE could be due to the changes occurring with aging in the molecular structure of the material. Such aging gradually does not allow the chains to re-orient and provide additional resistance following the initial yield of the material.²⁰ In fact, changes in the molecular structure associated

with the aging behavior are due to increased cross-linking and chain scission.¹⁻⁶ It was established already that in specimens exposed to radiation, side chain bonds are broken and become sites for cross-linking. Increasing the degree of crosslinking inhibits relative chain motion, strengthens the polymer and makes it more brittle.²⁹⁻³¹ Such interpretation for the deterioration in the mechanical behavior due to chain scission and associated reduction in the molecular weight can be correlated with the increases free surface energy. It can also be correlated with the initial reduction in the yellow color due to additives migration to the film surface and its diminishing before the yellow color starts to increase due to the effect of deterioration.

The limit of use/life time

It was reported in the literature that, the life time of a film used as greenhouse cover is based on the loss of its physicochemical and mechanical properties.^{14,32,33} Briassoulis et al.³⁴ showed that, if the film loses 50% of one of its properties, it becomes then unusable. It was shown that the UV light effects on a LDPE film are observable for an aging of 5 months.²⁶

To get the limit of use service time based on the 50% loss in the initial film property criterion, one can draw the variation of the normalized property with the aging time. Normalizing the property with the initial value of the unaged film and plotting it with aging time will provide information about the limit of use service time under each aging condition. but also will provide a deep The property To get deep insight on the effect of the aging time on the mechanical performance of the film under the different aging conditions, one can compare the film property value after exposure to aging conditions and its corresponding property value of the unaged material. This will also provide information about the limit of use service time according to the criterion of the 50% loss in the original property. Such variation can be done for each mechanical property. Figure 10 shows the standard curves of the variation of the normalized elasticity modulus E and strain at break (fracture strain ϵ_f) under different aging conditions (natural, 40°C, 40°C + UV-A, 50°C and 50°C + UV-A) with aging time. The two properties are normalized with their values for the unaged film (E_{unaged} and $\epsilon_{f, \text{unaged}}$). Figure 10 shows that all strains at fracture curves intersect with the horizontal line that represent the 50% reduction in the initial property excepting that for naturally aged and artificially aged at 40°C films. Therefore, these two curves are hypothetically extrapolated up to aging time of 9000 h (12.5 months) and 7299 h (10 months), respectively to enable the life time to be predicted under these

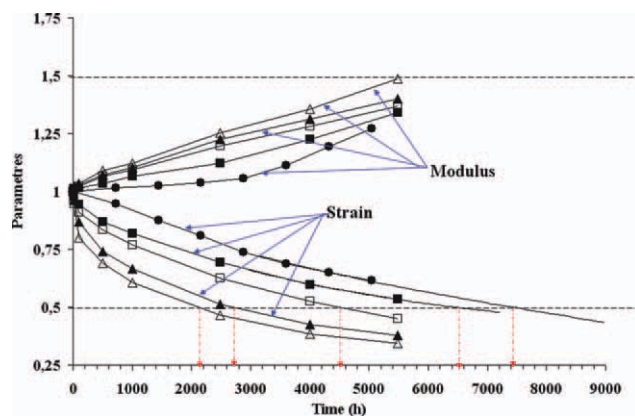


Figure 10 Evolution of the normalized elasticity modulus and elongation at break with the aging time (● natural, ■ 40°C, □ 40°C + UV-A, ▲ 50°C, and △ 50°C + UV-A). [Color figure can be viewed in the online issue, which is available at wileyonlinelibrary.com]

two aging conditions. It is noticed from these curves that the strain at break for all artificially aged films reduces to 50% of the unaged film value before their elasticity modulus increases with 50% of the unaged film value. The naturally aged film reaches its limit of use time at 7500 aging hours. On the other hand, the limit of use times of the artificially aged films at 40°C, 40°C + UV-A, 50°C, 50°C + UV-A takes place at 6550, 4500, 2750, and 2100 h, respectively. The results reflect that the aging deteriorative impact on the ductility and flexibility increases with aging time. Also, the limit of use service time reaches its lowest value for films exposed to UV radiation and 50°C.

It is also of importance to determine the normalized value of the property at the end of aging time and plot it with the aging condition. This helps in comparing between the levels of the deteriorative impact of the five aging conditions on the normalized property at the end of aging periods. It is also important comparing the values of the deteriorative effect of the five different aging conditions on the mechanical property of the LDPE tri-layer film at the end of aging periods with its initial value for each aging condition. The values of the normalized mechanical properties at the end of aging time (5040 h/7 months in natural aging and 5486 h/7.6 months in artificial aging) under different aging conditions are summarized and presented in Figure 11. Each mechanical property is normalized with its corresponding value for the unaged film (virgin material). The stress at the first peak or at the point of zero slope was considered as the yield strength. The curves of all properties are decreasing excepting the elasticity modulus which is increasing. The increase in the elastic modulus is a sort of degradation as it is an indication for a reduction in the film flexibility. It is worth noting here that, the curves of the yield

strength, fracture stress and fracture strain are identical and coincident. This means that the percentage loss in each mechanical property with respect to the value for unaged film is approximately equal for all aging conditions. It is also observed that the line joining between the property values under natural aging and artificial aging at 40°C is almost horizontal. In fact, the effect of natural aging on the properties is almost equivalent to that of the artificial aging at 40°C. Further, the exposure up to the end of the natural aging period (5040 h) and up to the end of artificial aging period at 40°C (5486 h) does not cause the 50% reduction in the property. However the end of service limit of use time was taken place under the other three aging conditions and the harshest effect is due to the exposure to 50°C with UV-A radiation.

Since the loss in the yellow color (day additive) can be correlated to the deterioration in the mechanical property. Therefore, it is worth to use it as a criterion to determine the limit of use service time of the film. It is expected that the loss of 50% of the initial intensity of the color may be a conservative criterion to measure the limit of use time, thus the validity of the maximum loss in the yellow color can be checked. Figure 12 shows the Limit of use time (in hours) based on the maximum loss in the yellow color and based on the 50% loss in ductility for the sake of comparison. It is shown that the maximum reduction in the two properties is due to the exposure to 50°C and UV-A radiation; 2100 h based on 50% loss criterion and 200 h based on total loss in the color criterion, respectively. The limit of use time based on the maximum loss of the yellow color criterion is much less than half of that based on 50% loss in the ductility criterion. Therefore, the maximum loss in the day additive based -criterion is very

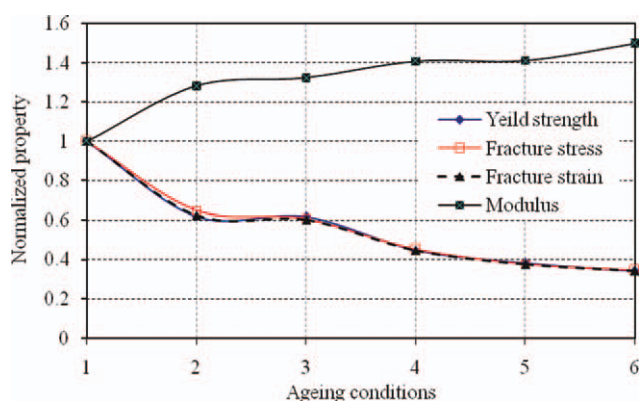


Figure 11 Normalized mechanical properties, at the end of aging time, versus aging condition. (1) Unaged; (2) natural aging; (3) aging at 40°C; (4) aging at 40°C + UV-A; (5) aging at 50°C; and (6) aging at 50°C + UV-A. [Color figure can be viewed in the online issue, which is available at wileyonlinelibrary.com]

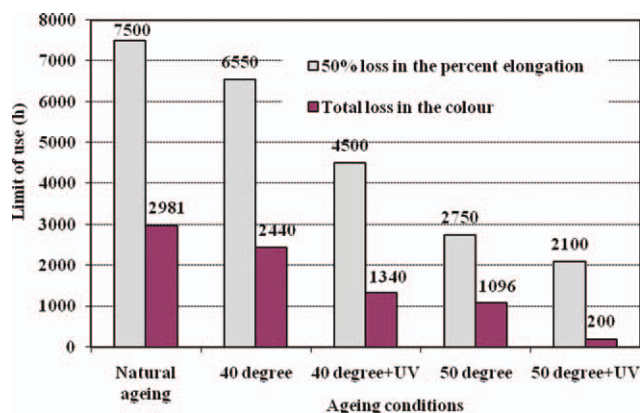


Figure 12 Film limit of use time based on 50% reduction in the strain to fracture (percent elongation) and the maximum loss of yellow color criteria versus aging conditions. [Color figure can be viewed in the online issue, which is available at wileyonlinelibrary.com]

conservative as the film hasn't yet lost 50% of its mechanical properties. As expected the limit of use service time under the exposure to natural aging is more than that under the exposure to artificial aging.

Thermal analysis

The LDPE is a semicrystalline polymer with a high degree of crystallinity. Among the advantages of semicrystalline polymers, compared with amorphous ones, is that their maximum use temperature is set by the melting (fusion) temperature rather than the glass transition temperature. DSC analysis was conducted to check the thermal stability and applicability of LDPE film as a greenhouse cover. Melting endotherms are used to thermally characterize the crystalline melting point (T_m) corresponding to the first heating of the unaged and aged LDPE films. The structural modification, if any, in LDPE films during aging can also be explained by DSC test results.

Figure 13 presents the DSC heating curves of unaged (virgin) and naturally aged samples for periods of 720 h (1 month), 2880 h (4 months), and 5040 h (7 months). The melting behavior of the unaged and naturally aged samples is almost similar. Two melting peaks were observed. The main or strong one occurred at 110°C and the secondary or weak one at 120.5°C for the unaged film. The two melting temperatures were shifted to lower temperatures (118.5 and 108°C) for the aged film.

During heating process in the DSC analysis of LDPE in references,^{33–35} the crystallinity is revealed by an endothermic peak of melting at a temperature T_m close to 100°C, where the characteristic temperature T_m is taken as the maximum of the endothermic peak of melting. Mourad et al.^{1,2} have observed a

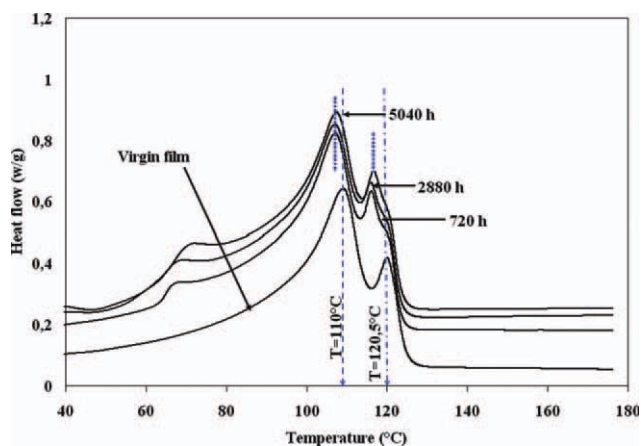


Figure 13 DSC thermograms of unaged LDPE film and aged naturally for periods of 720, 2880, and 5040 h. [Color figure can be viewed in the online issue, which is available at wileyonlinelibrary.com]

crystallinity melting temperature of 100.5°C for VLDPE. They have also observed that, it remained almost constant up to 7 days of oven aging at 100°C and it increased by 2°C after 14 days of aging. Khabbaz and Albrtsson³⁶ have observed that the unaged LDPE has T_m of 110°C which equal to the observed T_m of the used LDPE.

Figure 14 presents the DSC melting curves of unaged and artificially aged samples at 40°C for periods of 500 h, 1000 h, 2480 h and 5486 h. The melting behavior of artificially aged samples is almost similar as unaged and naturally aged sample, i.e., the shape of the melting peaks is analogous. The two melting temperatures (strong and weak ones) were shifted to lower temperatures by at the most 3.5°C. The DSC curves for other three aging conditions (40°C + UV-A, 50°C, and 50°C + UV-A) were obtained. The results are similar as for 40°C. It is

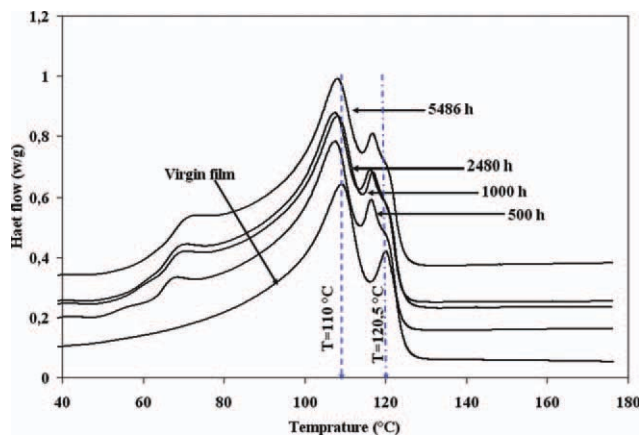


Figure 14 DSC thermograms of unaged LDPE films and aged artificially at 40°C for periods of 500, 1000, 2480, and 5486 h. [Color figure can be viewed in the online issue, which is available at wileyonlinelibrary.com]

TABLE IV
 T_m of the Strong and Weak Peaks Under Different Artificial Aging Conditions

Aging condition	Aging period									
	Unaged		500 h		1000 h		2480 h		5486 h	
	Strong	Weak	Strong	Weak	Strong	Weak	Strong	Weak	Strong	Weak
40°C	110°C	120.5°C	108°C	118°C	107.5°C	117°C	107.5°C	117°C	107.5°C	118°C
40°C + UV-A	110°C	120.5°C	107.5°C	118°C	107°C	117°C	106.5°C	116.5°C	107°C	117°C
50°C	110°C	120.5°C	107°C	117°C	107°C	117°C	106.5°C	116.5°C	106.5°C	116.5°C
50°C + UV-A	110°C	120.5°C	107°C	117°C	107°C	117°C	107°C	116.5°C	106.5°C	116.5°C

therefore, not necessary to include these curves. Table IV shows the T_m (of the strong and weak crystallinity melting peaks) values for unaged and all artificial aging conditions.

The calorific curves for the melting region of LDPE were obtained for unaged and aged materials at 60°C and 100°C for period of 14 days by Khabbaz and Albrtsson.³⁶ They have observed that the melting temperatures for the three cases were 110°C, 110°C, and 115°C, respectively and the melting peak became smaller and sharper after aging at 100°C. They reported that these changes in the melting peaks and melting temperature are probably attributed to the formation of more uniform and perfect crystals during the degradation, and these melt at higher temperature. These observations were for one layer LDPE films with thicknesses of 37 μm .

The DSC results show that, during the aging of this material (over a period of 5486 h.) the melting behavior hasn't changed and there is a minor change in T_m and consequently the bulk crystalline structure of the three layers sheet hasn't modified. More interesting is the shape of the signal, which exhibits two clear endothermic peaks of melting close to each other (difference is about 10°C for all periods of natural and artificial aging). The presence of at least two types of crystalline structures is expected, but the interpretation of this data must be investigated carefully. The existence of three layers and two interfaces between the three layers is able to modify drastically the heat flux transfer inside the samples and it must be kept in mind that LDPE is more an insulator rather than a conductor. So that, some delay time in the heat flux transfer may occur leading to the appearance of two peaks.³⁷

If the aging does not modify the structural property of the crystalline phase, it remains that the modifications of the interfaces and/or of the vitreous phase must explain the mechanical modifications observed during aging. Carrasco et al.³⁸ indicated that the structural modifications and chemical changes, for this type of materials, are complex. Certain changes lead to a crystallinity increase and others to a crystallinity decrease. A non-destructive analysis of the interfaces is relatively complex excepted for the two exterior sides. For these the

characterization of the surface was performed by measuring the free surface energy.

FTIR analysis

Infrared (IR) analysis was conducted to find out the nature and the cause of the degradation if any. Figure 15 shows FTIR spectra of unaged and naturally aged film tri-layers. The samples were taken from the outside face of the northern side of the greenhouse. The spectrum of non-aged film shows the presence of the traditional absorption bands of polyethylene. These are: at 2849 cm^{-1} and 2920 cm^{-1} which correspond to the vibration mode of the chain CH_2 groups, at 1430 cm^{-1} and between 720 and 850 cm^{-1} (low intensity) correspond to deformation and elongation mode of CH_2 group.^{39,40} During aging we observed that for the outside face of the film (exposed to UV radiation) the absorption bands (at 1430 cm^{-1} , 2920 cm^{-1} , 2849 cm^{-1} and between 720 cm^{-1} and 850 cm^{-1}) do not vary, and on the other hand after the first month (March) a peak at 900 cm^{-1} –1040 cm^{-1} has appeared which corresponds to the large absorption band of vibrations of $\text{CH}_2\text{-O}$ group or $\text{C}=\text{C}$ double bond.⁴¹ The maximum intensity of this peak is reached in July. This is due to the breaking and branching of double bonds under

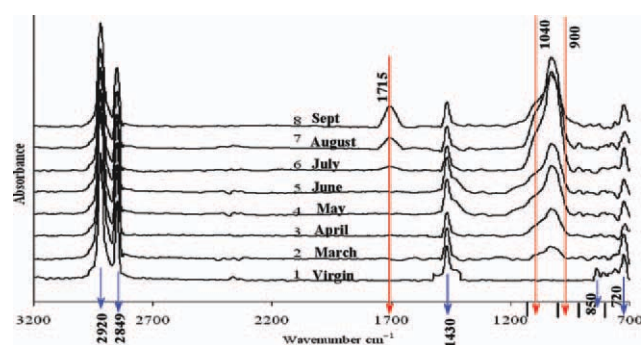


Figure 15 Infrared spectra of unaged and naturally aged trilayers films. The sample has been taken from the outside face of the northern side of the greenhouse (1) virgin film; (2) 1 month; (3) 2 months; (4) 3 months; (5) 4 months; (6) 5 months; (7) 6 months; and (8) 7 months. [Color figure can be viewed in the online issue, which is available at www.interscience.wiley.com] www.interscience.wiley.com]

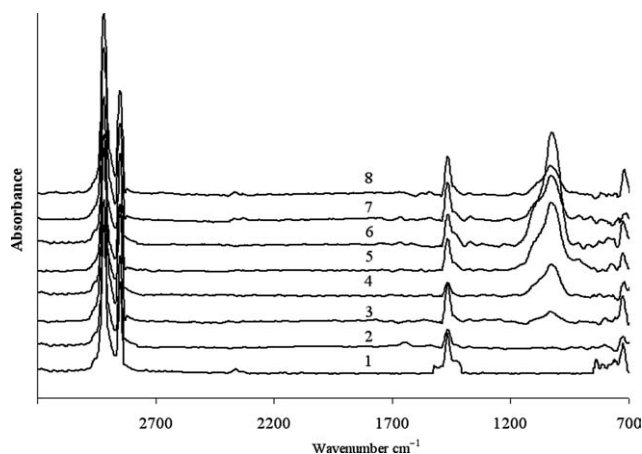


Figure 16 Infrared spectra of unaged and naturally aged trilayers films. The sample has been taken from the inside face of the northern side of the greenhouse (1) virgin film; (2) 1 month; (3) 2 months; (4) 3 months; (5) 4 months; (6) 5 months; (7) 6 months; and (8) 7 months.

natural aging. Also a new peak at 1715 cm^{-1} appears at similar time (July), which corresponds to the bands of vibrations of the $\text{C}=\text{O}$ functions. The carbonyl groups characteristics of the chain photo-oxidation are deduced from band at 1715 cm^{-1} . This is the band that increases more considerably with the irradiation time. The presence of these two last absorption bands (at $900\text{--}1040\text{ cm}^{-1}$ and at 1715 cm^{-1}) confirm the presence of $\text{CH}_2\text{--O}$, $\text{C}=\text{C}$ and $\text{C}=\text{O}$ functions on the surface of the film tri-layers, undoubtedly related to the degradation due to chemical aging. Indeed, under the action of the light and/or heat there is formation of radicals on the film surface, which lead to reactions of reticulation of chains, reactions with oxygen in air and reactions of scission of chains.

The FTIR spectra was also obtained for samples taken from the inside face of the film. The Infrared spectra are demonstrated in Figure 16. It is worth noting here that, the bands at $720\text{--}850\text{ cm}^{-1}$, 1040 cm^{-1} , 2849 cm^{-1} , and 2920 cm^{-1} of the outside face

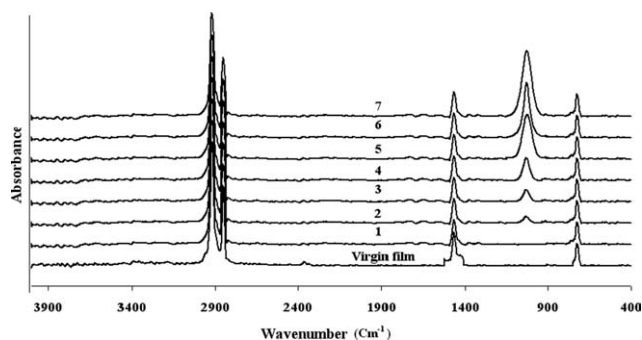


Figure 17 Infrared spectra of unaged and artificially aged trilayers film at 40°C . The samples taken from the inside face of the film. (1) 20 h; (2) 100 h; (3) 500 h; (4) 1000 h; (5) 2460 h; 4000 h; and (7) 5486 h.

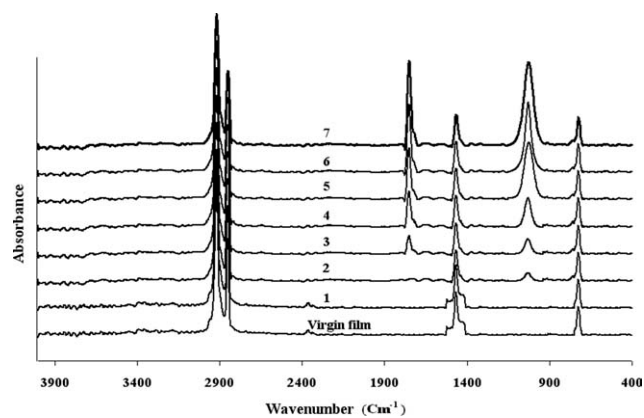


Figure 18 Infrared spectrum of unaged and artificially aged trilayers film at $40^\circ\text{C} + \text{UV-A}$. (1) 20 h; (2) 100 h; (3) 500 h; (4) 1000 h; (5) 2460 h; (6) 4000 h; and (7) 5486 h.

sample are observed for the inside film sample with the total absence of the band at 1715 cm^{-1} which appeared after July for the outside sample. Jin et al.¹⁴ reported that fractions UV of the solar radiation are absorbed by the yellow dye or the additives anti-UV present in the film, progresses with the penetration in the thickness of the film. The luminous energy received on the inside face of the film does not seem sufficient to cause reactions of photo-oxidation. It is also necessary to take account of the difference in atmosphere, the rain, the sand storms, etc. The tests results showed that, whatever the place, on the film side, of taking of the samples, the spectra FTIR are identical.

The IR absorption spectra of tri-layer films exposed to artificial periods ranging from 20 to 5486 h and to the four studied conditions of heat and UV radiation are presented in Figures 17–20 respectively. The spectrum of unaged film is included in all curves for the purpose of comparison. In all artificial aging conditions and as in the natural aging, the traditional absorption bands of polyethylene: 2849 cm^{-1} and 2920 cm^{-1} correspond to the vibration mode of the chain of CH_2 groups (at 1430 cm^{-1}

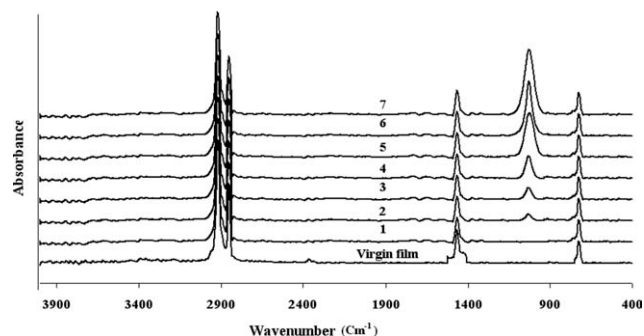


Figure 19 Infrared spectra of unaged and artificially aged trilayers film at 50°C . (1) 20 h; (2) 100 h; (3) 500 h; (4) 1000 h; (5) 2460 h; (6) 4000 h; and (7) 5486 h.

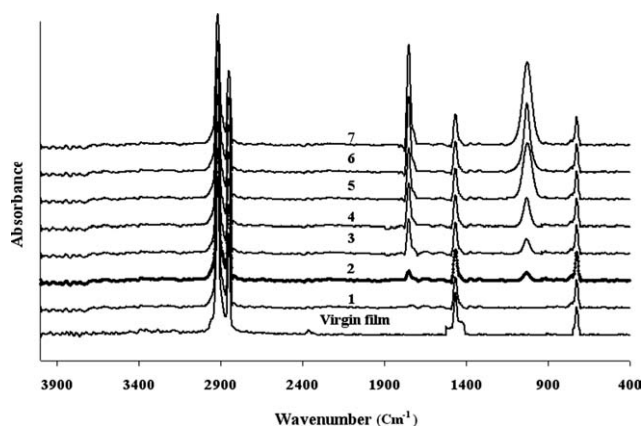


Figure 20 Infrared spectra of unaged and artificially aged trilayers film at 50°C + UV-A. (1) 20 h; (2) 100 h; (3) 500 h; (4) 1000 h; (5) 2460 h; (6) 4000 h; and (7) 5486 h.

and between 720 and 850 cm^{-1} , low peak intensity, correspond to the deformation and elongation mode of CH_2 groups are shown). Also, the absorption band at 1430 cm^{-1} (and also at 2849 and 2920 and at 720–850) were unaltered, even under the exposure to UV-A. It is worth noting here that there is a total absence of the band at 1715 cm^{-1} under exposure to heat only (at 40 and 50°C) as in the case of the natural aging of the sample taken from the inside surface of the greenhouse. A peak at 900–1040 cm^{-1} appears after 500 h of exposure to 40°C (Fig. 17) and 100 h of exposure to 40°C + UV-A, 50°C and 50°C + UV-A (Figs. 18–20). This peak was also observed after one month (March) of natural aging corresponding to the vibration of the $\text{CH}_2\text{-O}$ groups⁴² or double bonds $\text{C}=\text{C}$.⁷ The maximum peak intensity of this band is reached at 5486 h, however the maximum peak intensity reached by the end of July in natural aging. This is resulting from the rupture of double bonds as a result of aging. Also a new peak at 1715 cm^{-1} appears after 500 h of exposure to temperature and UV-A radiation, which corresponds to the bands of vibrations of the $\text{C}=\text{O}$ functions. This band was also observed in natural aging of the sample taken from the outside surface of the greenhouse at the end of July. As mentioned in the preceding section, the carbonyl groups characteristics of the chain photo-oxidation are deduced from band at 1715 cm^{-1} , which is the band that increases more considerably with the irradiation time. Further, the presence of these two last absorption bands (at 900–1040 cm^{-1} and 1715) confirms the presence of $\text{CH}_2\text{-O}$, $\text{C}=\text{C}$ and $\text{C}=\text{O}$ functions on the surface of the tri-layer film, undoubtedly related to the degradation due to chemical aging.

The degradation model of LDPE used in this study was shown by Tidjani.⁷ Indeed, under the action of the light and/or heat there is formation of radicals on the film surface, that leads to reactions of

reticulation of chains, reactions with oxygen in air and reactions of scission of chains. These observed three types of reactions (in both natural and artificially aging) can coexist. The prevalence of a mode of degradation with respect to another depends on the nature and the stability of the radical formed in the course of the reaction of photo-oxidation.⁴³ In the case of LDPE the tertiary carbons (20–40 carbon atoms/1000) can lead to stable radicals. They are likely to react with other radicals and lead to reticulations of the chains. The secondary carbons lead to very reactive radicals and cause reactions of chains scission.⁴⁴

The FTIR results strengthen the previous results of the increase in the free surface energy, the changes in the yellow color and the deterioration in the mechanical properties due to aging.

CONCLUSION

The impact of natural and artificial aging on the characteristics of the tri-layer LDPE film used as a greenhouse roof was investigated. Aging causes an increase in the free surface energy due to the chemical modification associated with exposure to UV radiation and temperature. The value characterizing the yellow color is 91% for unaged film. It decreases at the beginning of the aging process and passes through a minimum. This is due to the migration of additives to the film surface. Then it starts to increase up to the end of aging periods which is attributed to the film degradation. The exposure to UV radiation and temperature has a deteriorative effect on the mechanical properties (modulus, yield strength, ductility). The DSC analysis show that there is small shift to a lower temperature in the T_m , however the aging has not affected the melting behavior. The DSC data show the presence of two types of melting peaks or crystalline structure because of the existence of three layers and the two interfaces between them. New two absorption bands at 900–1040 cm^{-1} and 1715 beside the traditional PE bands (at 2849 cm^{-1} , 2920 cm^{-1} , 1430 cm^{-1} and between 720 and 850 cm^{-1}) are observed in the IR spectra. These two bands confirm the presence of $\text{CH}_2\text{-O}$, $\text{C}=\text{C}$ and $\text{C}=\text{O}$ functions on the surface of the tri-layer film, due to its degradation. The peak at 900–1040 corresponds to the vibration of the $\text{CH}_2\text{-O}$ groups or double bonds $\text{C}=\text{C}$ resulting from the rupture of double bonds as a result of natural and artificial aging. The peak at 1715 cm^{-1} corresponds to the bands of vibrations of the $\text{C}=\text{O}$ functions. The carbonyl groups characteristics of the chain photo-oxidation are deduced from band at 1715 cm^{-1} . There is a total absence of the band at 1715 cm^{-1} under exposure to heat only in the artificial aging as in the

case of the natural aging of the sample taken from the inside surface of the greenhouse.

Generally, the natural aging of the film in North Africa is almost equivalent to artificial aging at 40°C. Further, the sunlight radiation is major element of degradation and the anti UV additives are not optimized in this film. The combined effect of the temperature and UV–A radiation reduces the life time considerably. The data of the free surface energy, yellow color, DSC, and FTIR are correlated with the degradation in the mechanical performance of the film.

NOMENCLATURE

E	modulus of elasticity
T_m	crystallinity melting temperature
σ , σ_f , σ_y	stress, fracture stress, yield strength
ε , ε_f , $\varepsilon\%$	strain, fracture strain, percent strain

References

- Mourad, A.-H., I. Mater Design 2010, 31, 918.
- Mourad, A.-H., I.; Akkad, R. O.; Soliman, A. A.; Madkour, T. M. Macromol Eng 2009, 38, 265.
- Mourad, A.-H., I.; Fouad, M. H.; Elleithy, R. Mater Design 2009, 30, 4112.
- Fouad, M. H.; Mourad, A.-H., I.; Barton, D. C. Macromol Eng 2008, 37, 346.
- Fouad, M. H.; Mourad, A.-H., I.; Barton, D. C. Polym Test 2005, 24, 549.
- Mourad, A.-H., I.; Bekheet, N.; Al-Butch, A.; Abdel-Latif, L.; Nafee, D.; Barton, D. C. Polym Test 2005, 24, 169.
- Tidjani, A. Polym Degrad Stab 2000, 68, 465.
- Sigbritt, K.; Minna, H.; Ann-Christine, A. Macromolecules 1997, 30, 7721.
- Briassoulis, D.; Waaijenberg, D.; Gratraud, J.; Von Elsner, B. J Agric Eng Res 1997, 67, 171.
- Dilara, P. A.; Briassoulis, D. J Agric Eng Res 2000, 76, 309.
- Briassoulis, D.; Aristopoulou, A. Polym Test 2001, 20, 615.
- Briassoulis, D.; Aristopoulou, A.; Bonora, M.; Verlodt, I. Biosyst Eng 2004, 88, 131.
- Adam, A.; Kouider, S. A.; Yousef, B.; Hamou, A.; Saiter, J. M. Polym Test 2005, 24, 834.
- Jin, C.; Christensen, P. A.; Egerton, T. A.; Lawson, E. J.; White, J. R. Polym Degrad Stab 2006, 91, 1086.
- Basfar, A. A.; Idriss, A. Polym Degrad Stab 2006, 91, 437.
- Hassini, N.; Guenachi, K.; Hamou, A.; Saiter, J. M.; Marais, S.; Beucher, E. Polym Degrad Stab 2002, 75, 247.
- Dilara, P. A.; Briassoulis, D. Polym Test 1998, 17, 549.
- Youssef, B.; Dehbi, A.; Hamou, A.; Saiter, J. M. Mater Design 2008, 29, 2017.
- Youssef, B.; Benzohra, M.; Saiter, J. M.; Dehbi, A.; Hamou, A. Acta Hort (ISHS) 2008, 801, 123.
- Operation manual for FAMAS, Interface measurement and analysis system, Contact angle measurement [Sessile Drop], Kyowa Interface Science Co., Ltd.
- Robert, J. G.; Carel, J. V. O. Adv Colloid Interface Sci 1987.
- Owens, D. K.; Went, C. J Appl Polym Sci 1969, 13, 1741.
- Dupre, A., Ed. Theorie mecanique de la chaleur; Gauthier-Villars: Paris, 1969, p 369.
- Fowkes, Ind Eng Chem 1964, 56, 40, and with the following Qwen Wendt model of equation 3 the samples free surface energy was calculated.
- Sanchis, M. R.; Blanes, V.; Blanes, M.; Garcia, D.; Balart, R. Eur Polym J 2006, 42, 1558.
- Braudrup, J.; Immergut, E. H., Eds. Polymer Handbook, Section A, 3rd ed.; John Wiley & Sons: New York, 1989; Chapter 6.
- Scoponi, M.; Cimmino, S.; Kaci, M. Polymer 2000, 41, 7969.
- Dehbi, A.; Bouaza, A.; Hamou, A.; Youssef, B.; Saiter, J. M. Mater Design 2010, 31, 864.
- Hall, C. An Introduction for Technologists and Scientists, 2nd ed.; Wiley: New York, 1989.
- Torres, A.; Colls, N.; Mendez, F. J Plast Film Sheet 2006, 22, 29.
- Callister, W. D. Materials Science and Engineering: An Introduction, 6th ed.; John Wiley: New York, 2003.
- Rabek, F. J. Photodegradation of Polymers. Physical Characteristics and Applications; Springer: Berlin, 1996.
- Scarascia-Mugnozza, G.; Schettini, E.; Vox, G. Biosyst Eng 2004, 87, 479.
- Briassoulis, D. Polym Degrad Stab 2006, 91, 1256.
- Khabbaz, F.; Albertsson, A.-C.; Karlsson, S. Polym Degrad Stab 1999, 63, 127.
- Khabbaz, F.; Albertsson, A. C. J Appl Polym Sci 2001, 79, 2309.
- Sebaa, M.; Servens, C.; Pouyet, J. J Appl Polym Sci 1993, 47, 1897.
- Carrasco, F.; Pagès, P.; Pascual, S.; Colom, X. Eur Polym J 2001, 37, 1457.
- Gisjsman, P.; Sampers, J. Polym Degrad Stab 1997, 58, 55.
- Allen, N. S.; Adge, M.; Houldsworth, D.; Rahman, A.; Catalina, F.; Fontan, E. Polym Degrad Stab 2000, 67, 57.
- Gulmine, J. V.; Janissek, P. R.; Heise, H. M.; Akcelrud, L. Polym Degrad Stab 2003, 79, 385.
- Hassini, N.; Guenachi, K.; Hamou, A.; Saiter, J. M.; Marais, S.; Beucher, E. Polym Degrad Stab 2002, 75, 247.
- Hanafi, A.; Paposolomontos, A. Biotechnol Adv 1999, 17, 183.
- Briassoulis, D. Polym Degrad Stab 2006, 91, 1256.